ISSN: 2277-9655
(I2OR), Publication Impact Factor: 3.785

IJESRT

INTERNATIONAL JOURNAL OF ENGINEERING SCIENCES & RESEARCH TECHNOLOGY

ENERGY MANAGEMENT AND IMPROVEMENT OF POWER QUALITY IN A MICROGRID BY THE COORDINATED CONTROL OF DECENTRALISED GENERATION INVERTERS

M.Mehatab*, I.Kumaraswamy
* Post Graduate Student, Sree Vidyanikethan Engineering College,Tirupati.
Assiatant Professor, Sree Vidyanikethan Engineering College.

ABSTRACT

The aim of this work is to improve the power quality for Distributed Generation (DG) with power storage system. A microgrid consists of several Decentralised Generations connected near the load. In this paper wind, PV array is used as primary generations and Proton Exchange Membrane Fuel Cell is used as a secondary DG. A storage battery is used as a backup to meet the demand. The microgrid is operated in grid connected mode and islanded mode. The control of DG inverters is based on hysteresis controller. An energy management algorithm is implemented using Kalman filter. A test scenario is presented under different conditions.

KEYWORDS: Decentralised Generation, energy management, hysteresis control.

INTRODUCTION

Quality of power supply is a major concern in the present days. Power quality is the combination of voltage quality and current quality. The main problems with low power quality are stationery and transient distortions in the line voltage such as harmonics, flicker, swells, sags and voltage asymmetries [1].

Distributed Generation (DG) also called as site generation, dispersed generation, embedded generation, decentralized generation, decentralized energy or distributed energy, generates electricity from the many small energy sources [2].

The existing method consisting of using PV array and fuel cell as decentralised generations, in this proposed model, DG is assumed to include Wind power Generation (WG) ,PV array and Proton Exchange Membrane Fuel Cells (FC). Advantages of this system are constant power supply, constant voltage magnitude, absence of harmonics in supply voltage, un-interrupted power supply. A lithium ion storage battery is used as a backup supply to meet the demand. The microgrid is operated in grid connected mode or islanded mode. Based on the state-of-charge (SOC) of storage battery an energy management algorithm is implemented using Kalman filter.

SYSTEM DESCRIPTION AND MODELLING

System Description

Fig. 1 shows the configuration of the proposed microgrid that is designed to operate either in the grid-connected or islanded mode. The main DG unit comprises of a 175W PV array, wind generation of 3 kW and a 50-kW PEMFC that are connected in parallel to the dc side of the DG inverter 1 through dc/dc boost converters to regulate the dc-link voltage of the DG inverter at the desired level by delivering the necessary power. The PV array and

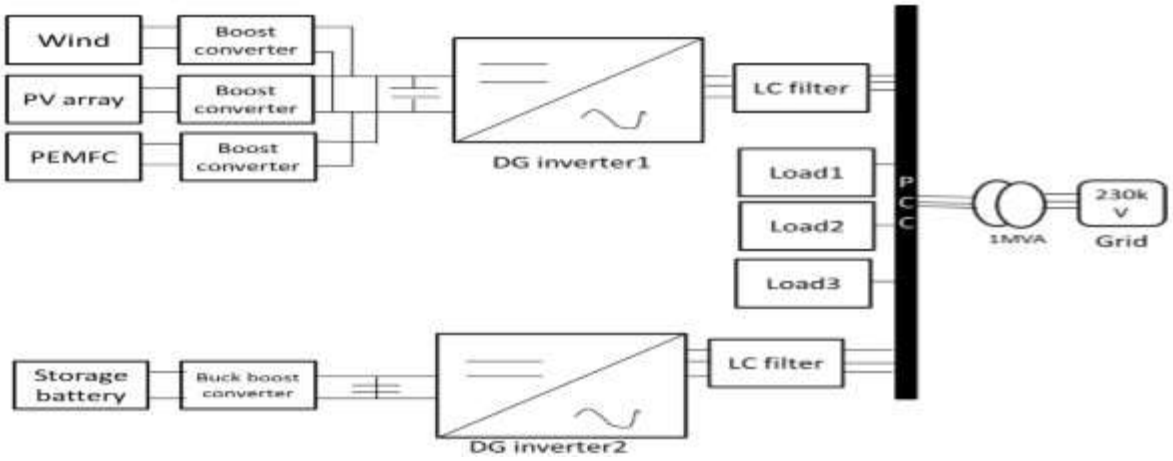

Fig.1 Basic block diagram of microgrid

wind generation is implemented as the primary generation unit and the PEMFC is used to back up the intermittent generation of the PV array. The maximum power generated by the wind turbine is P_{wg} ,the maximum power delivered by the PV array is P_{pv}. To maintain the level of the dc-link voltage at the required level, the PEMFC supplements the generation of the PV array to deliver the necessary P_{fc}. A 30-Ah lithium-ion SB is connected to the dc side of DG Inverter2 through a bidirectional dc/dc buck-boost converter to facilitate the charging and discharging operations. During islanded operation, the role of the SB is to maintain the power balance in the microgrid which is given by

$$P_{DG}+P_b=P_L \quad (1)$$

where P_{DG} is the power delivered by the main DG unit, P_b is the SB power which is subjected to the charging and discharging constraints given by

$$P_b \leq P_{b,max} \quad (2)$$

and P_L is the real power delivered to the loads. The energy constraints of the SB are determined based on the state-of-charge (SOC) limits which are given as

$$SOC_{min}<SOC\leq SOC_{max} \quad (3)$$

Although the SOC of the battery cannot be measured directly, it can be determined through several estimation methods [3].When the microgrid operates islanding from the distribution grid, the SB can operate in the charging/discharging/idle mode depending on its SOC grid. The flowcharts in Figs. 2 and 3 summarize the operation of SB, based on the output information provided by an energy management system (EMS) during grid-connected and islanded operation respectively.

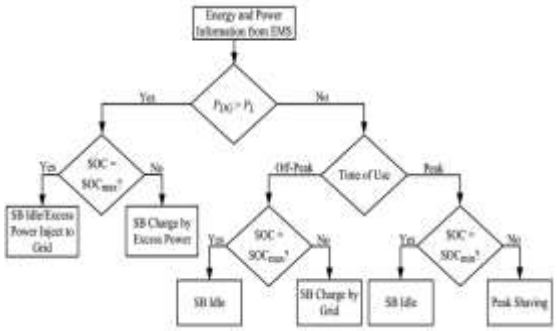

Fig.2 Operation of the SB during grid mode

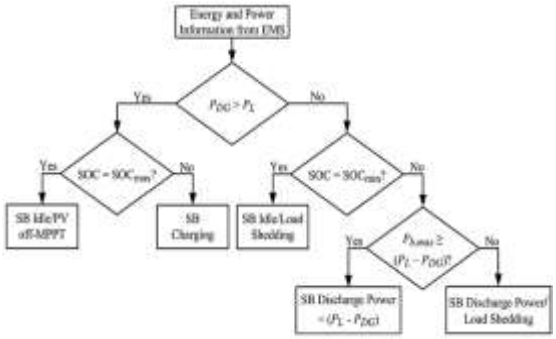

Fig.3 Operation of the SB during islanded mode

DG inverter modelling.

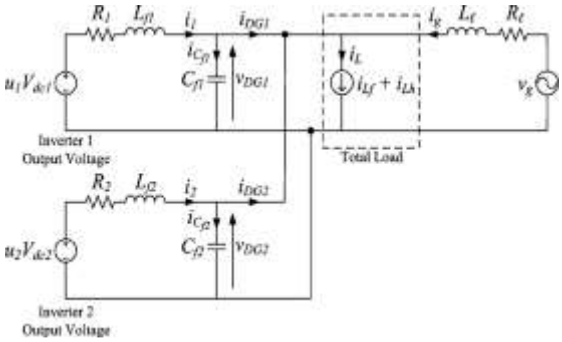

Fig.4 Equivalent single-phase representation of the DG inverters for grid connected operation.

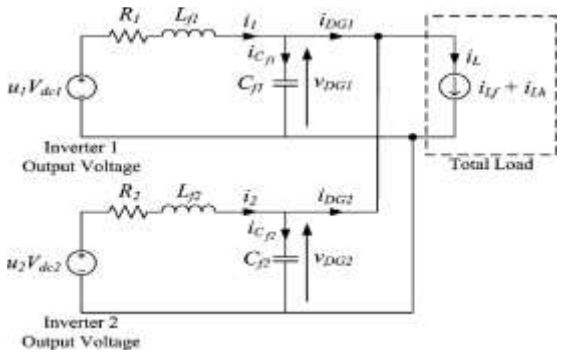

Fig.5 Equivalent single-phase representation of the DG inverters for islanded operation.

The EMS controls and monitors different aspects of power management such as load forecasting, unit commitment, economic dispatch, and optimal power flow through a centralized server. During grid-connected operation, the distribution grid is connected to the microgrid at the point of common coupling (PCC) through a circuit breaker

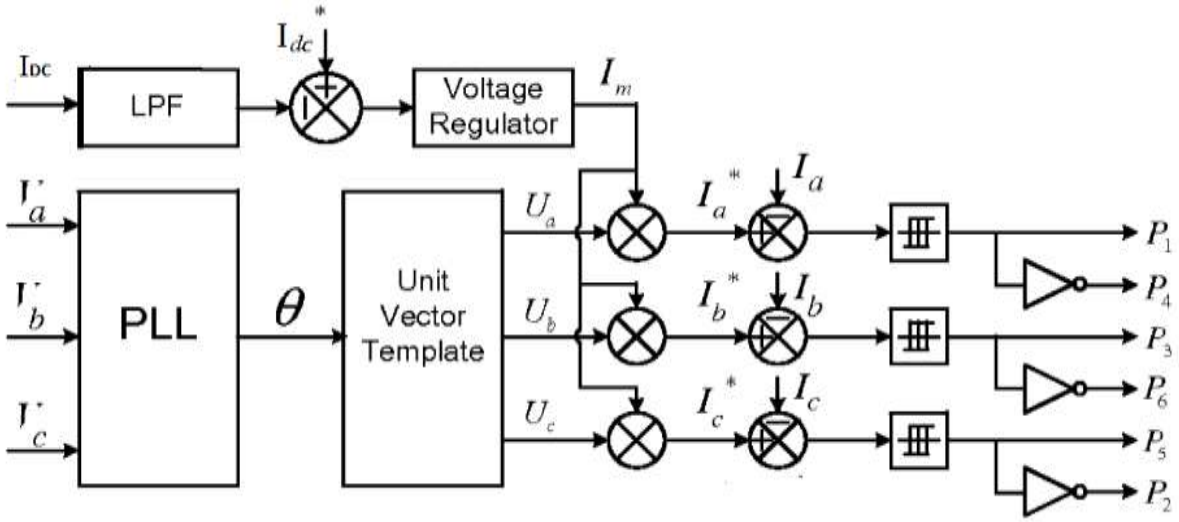

Fig.6 Block diagram representation of grid-interfacing inverter control

The role of the main DG unit is to fulfil the function of facilitating the local power and voltage to support the loads, thereby reducing the burden of generating and delivering power directly from the distribution grid. The DG units also takes the role of compensating the harmonics, if any, in the currents drawn by nonlinear loads in the microgrid, thus blocking the propagation of harmonics to other electrical networks connected to the PCC.

Figs. 4 and 5 show the equivalent single-phase representation of the DG inverters for grid-connected and islanded operation respectively [4]. The switched voltage across the output of the j^{th} DG inverter is represented by u_j,V_{DCj}, where u_j is the control input and j=1, 2. The output of the DG inverter is interfaced with an LC filter represented by L_{fj} and C_{fj} to eliminate the high switching frequency harmonics generated by the DG inverter.The resistance Rj models the loss of the DG inverter. The total load current, which is the sum of the currents delivered to the load (K=1, 2, 3), is given by:

$$iL = \sum_{K=1,2,3} iLk = iL1 + iL2 + iL3 \qquad (4)$$

and can be modeled as two components consisting of fundamental *iLf* and harmonic *iLh* with their peak amplitudes I_{Lf} and I_{Lh} , respectively, and is represented by

$$i_L = i_{Lf} + i_{Lh} = I_{Lf}\sin(\omega t - \varphi_{Lf}) + \sum_{K=1,2,3} iLh = \sin(h\omega t - \varphi Lh) \qquad (5)$$

$$= I_{Lf}\sin\varphi_{Lh}\cos\varphi_{Lf} - ILf\cos\omega t\sin\varphi_{Lf} + \sum_{K=1,2,3} iLh = \sin(h\omega t - \varphi Lh) \qquad (6)$$

$$= i_{Lf,p} + i_{Lf,q} + i_{Lh} \qquad (7)$$

Where φ_{Lf} and φ_{Lh} are the respective phase angles of the fundamental and harmonic components of i_L, and $i_{Lf,p}$ and $i_{Lf,q}$ are the instantaneous fundamental phase and quadrature components of i_L . To achieve unity power factor at the grid side, compensate for the harmonics in the load currents and simultaneously achieve load sharing. The inverter of the DG unit supplies a current i_{DGj} that is given by

$$i_{DGj} = (i_{Lf,p} - i_g) + i_{Lf,q+iLh} \qquad (8)$$

where i_g is the grid current. As shown in Fig.4, the distribution grid is supplied by a utility substation represented by a voltage source v_g during grid-connected operation, and is connected to the microgrid and the loads via a distribution line with resistance R_l and inductance L_l.

In the grid-connected mode, the grid voltage is known and the microgrid shares the load demand with the grid. Hence, to control the power delivered to the loads, the output current of the DG inverter is controlled using the current control

mode (CCM). During islanded operation, the microgrid will supply the overall load demand as shown in Fig. 5, and it is required that the output voltage be regulated to a pure sine wave of constant magnitude.

CONTROL DESIGN

The voltage source inverter is a key element of a DG system as it interfaces the photovoltaic energy sources generate power at low variable dc voltage. Thus, the power generated from these renewable sources needs power connected to a dc-link. The control diagram of grid- interfacing inverter for a 3-phase 3-wire system is shown in Fig. 6 [5].

The main aim of proposed approach is to regulate the power at PCC during: 1)P_{DG}=0; 2)P_{DG}<P_L; and 3)P_{DG}>P_L. While executing the power management operation, the inverter is actively controlled in such a way that it always draws/ supplies fundamental active power from/ to the grid. If the load connected to the PCC is non-linear or unbalanced or a combination of both, then the given control approach also compensates the harmonics, unbalance, and neutral current. The duty ratio of inverter switches are varied in a power cycle such that the combination of load and inverter injected power appears as balanced resistive load to the grid. The output of dc-link voltage regulator results in an active current (I_m).The multiplication of active current component with unity grid voltage vector templates (U_a, U_b and U_c) generates the reference grid currents (I_a^*, I_b^* and I_c^*). The grid synchronizing angle obtained from the phase locked loop (PLL) is used to generate unity vector template as

$$U_a=\sin\theta \quad (9)$$

$$U_b=\sin\left(\theta-\frac{2\pi}{3}\right) \quad (10)$$

$$U_c=\sin\left(\theta+\frac{2\pi}{3}\right) \quad (11)$$

The actual dc-link voltage (I_{dc}) is sensed and given to Park's transformation to reduce the complexity and then passed through a first-order low pass filter (LPF) to eliminate the presence of switching ripples on the dc-link voltage and in the generated reference current signals. The difference of this filtered dc-link voltage and reference dc-link voltage (I_{dc}^*) is given to a discrete- PI regulator to maintain a constant dc-link voltage under varying generation and load conditions. The dc-link voltage error ($I_{dcerr(n)}$) at nth sampling instant is given as:

$$I_{dcerr(n)}=I_{dc}^*(n)-I_{dc}(n) \quad (12)$$

The instantaneous values of reference three phase grid currents are computed as

$$I_a^*=I_mU_a \quad (13)$$
$$I_b^*=I_mU_b \quad (14)$$
$$I_c^*=I_mU_c \quad (15)$$

The reference grid currents (I_a, I_b and I_c) are compared with actual grid currents (I_a^*, I_b^* and I_c^*) to compute the current errors as

$$I_{aerr}=I_a^*-I_a \quad (16)$$
$$I_{berr}=I_b^*-I_b \quad (17)$$
$$I_{cerr}=I_c^*-I_c \quad (18)$$

These current errors are given to hysteresis controller. The hysteresis controller generates the gate pulses. Kalman filter [6] is used as predictor for proper energy management.

SIMULATION STUDIES

Table I Parameters of the Proposed System

Parameter	Value
Distribution grid voltage	22kV
DC link voltage	400V
Distribution line impedance	R_f=0.0075Ω,L_f=25.7μH
LC filter	L_f=1,2mH,C_f=20μF
DG inverter loss resistance	R_f=0.01Ω
Solar rating	175W
PEMFC	50kW
Wind Generation	3kW
Storage battery	30Ah

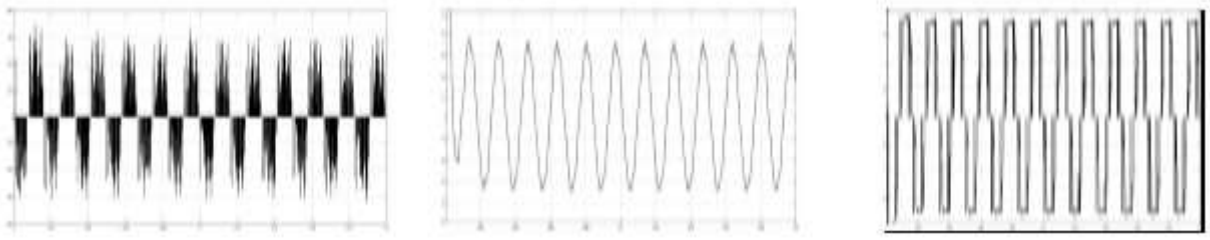

Fig.7 Per-phase currents drawn by loads 1,2, and 3.

The simulation model of the microgrid shown in Fig. 1 is realized in Matlab/Simulink. Three different load types consisting of linear and nonlinear loads are considered in the studies. For load 1, a 15-kVA three-phase PWM adjustable speed drive (ASD) is used and load 2 is made up of a three-phase RL load rated at P_{L2}=28 kW and Q_{L2}=18.5 kVAr, load 3 is a noncritical three-phase dimmer load rated at P_{L3}=18 kW and Q_{L3}= 12.3 kVAr, which is nonlinear in nature and will be shed under emergency conditions when the generation of the microgrid is unable to meet the load demand.

Test case 1: Power Quality Improvement by Placing a Wind Generation

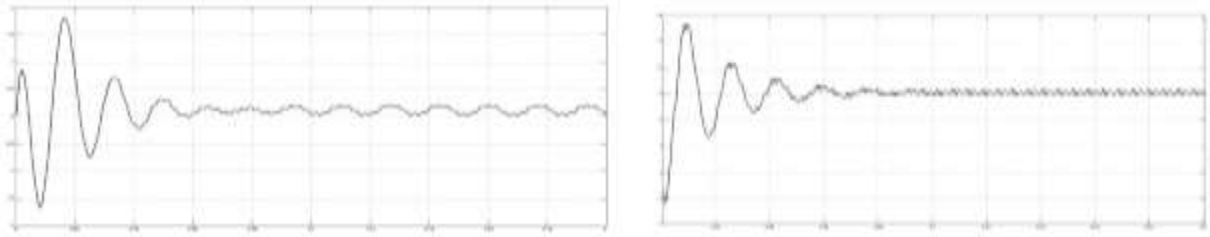

Fig.8 Real (left) and reactive (right) power delivered by the Grid before placing wind generation.

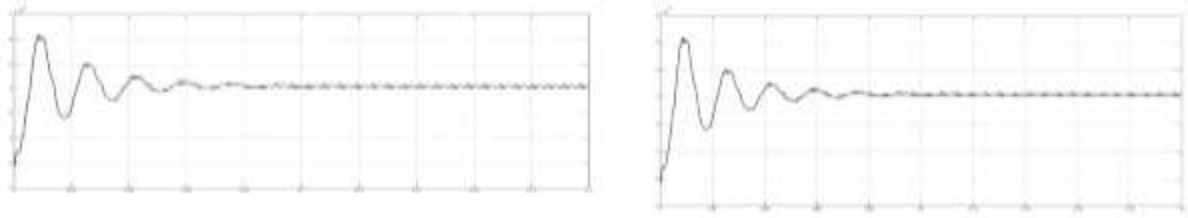

Fig.9 Real (left) and reactive (right) power delivered by DG before placing wind generation

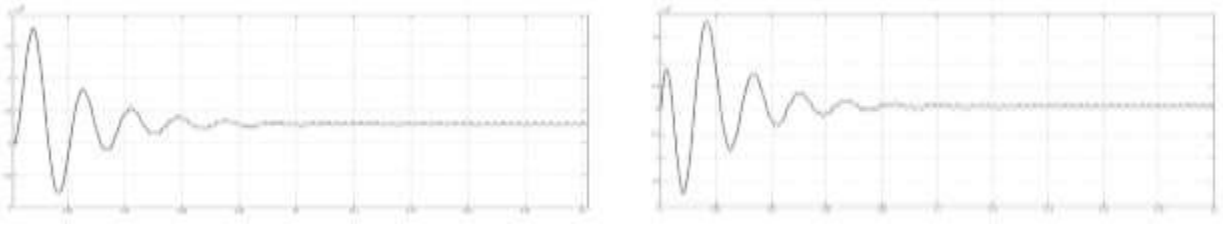

Fig.10 Real (left) and reactive (right) power delivered by the grid after placing wind generation.

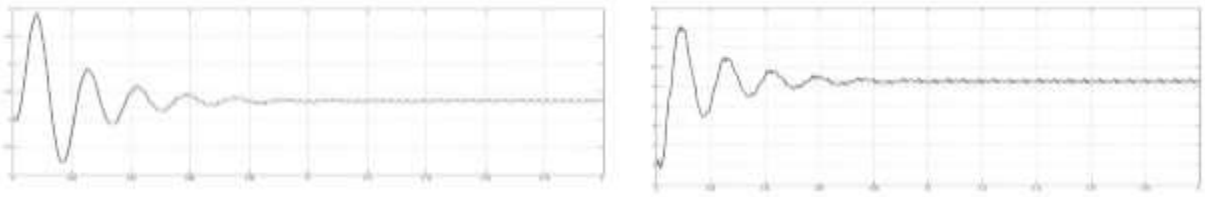

Fig.11 Real (left) and reactive (right) power delivered by DG after placing wind generation.

The Fig.8 and Fig.9 shows the real and reactive power waveforms of grid and DG before placing a wind generation. The Fig.10 and Fig.11 shows the real and reactive powers of grid and DG. The simulation is run for $0 \leq t < 0.2$s to reduce the simulation time. The first test case demonstrates the capability of the microgrid to improve the power quality of the distribution network by compensating for the harmonics in the total load current due to the nonlinear loads that are connected to the distribution network, such that the harmonics will not propagate to the rest of the distribution network during grid-connected operation. In this test case, the main DG unit accounts for 20% of the total load demand. The total real and reactive power delivered to the loads is about 58 kW and 35 kVAr. The SB is operating in the charging mode to store energy during off-peak period where the cost of generation from the grid is low to meet future sudden demands for power. The real power dispatched by the main DG unit is 11.6 kW (20% of the real power consumed by the loads) as shown in Fig.9, then increases to 30kW after placing wind generation which demonstrates the capability of the main DG unit to dispatch the required power and the power quality is also improved by reduction of ripples as shown in Fig.11. The main DG unit also delivers all of the reactive power required by the loads to achieve unity power factor at the grid side. The real and reactive power delivered by the grid after placing wind generation is shown in Fig. 10. It can be observed from Fig. 10 that the grid supplies 80% (46.4 kW) of the total real power delivered to the loads and dispatches an additional power of about 3 kW to charge the SB. It is also observed that the reactive power supplied by the grid is zero, resulting in unity power factor at the grid side. The real and reactive powers consumed by the loads remains constant after placing wind generation. From the figures it can be observed that the number of harmonics reduced after placing a wind generation.

Test Case 2: Peak Shaving of Loads during Peak Periods

The electricity pricing in many countries is impacted by the TOU tariffs. In DSM, energy-storage devices can be used to reduce the burden of generation of power directly from the distribution grid during peak periods. The second test case demonstrates the operation of the microgrid to achieve peak shaving in order to reduce the cost of generation from the grid when consumers practice DSM.

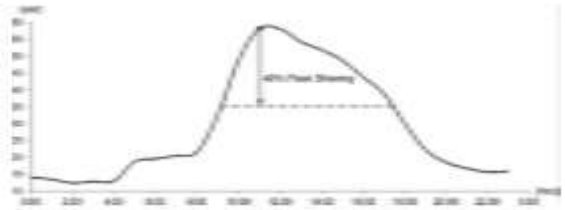

Fig.12 Hourly demand response curve.

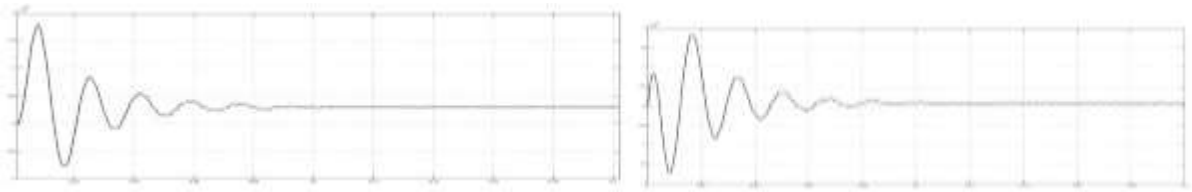

Fig.13 Real (left) and reactive (right) power delivered by the grid.

Fig. 12 shows a typical hourly demand response curve in a day indicated by the solid line. As in test case 1, the main DG unit is controlled to deliver 20% of the load demand. To achieve peak shaving at 11:00 h, the SB is operating in the discharge mode to provide 20% (11.6 kW) of the load demand. It can be seen from Fig. 13 that the real power delivered by the grid is 60% (34.8 kW) of the load demand with peak shaving, and the reactive power supplied is zero with the main DG unit compensating for the reactive components of the load currents. The SB delivers the required real power of about 20% (11.6 kW) of the load demand during peak shaving.

Test Case 3:Load Shedding During Islanded Operation

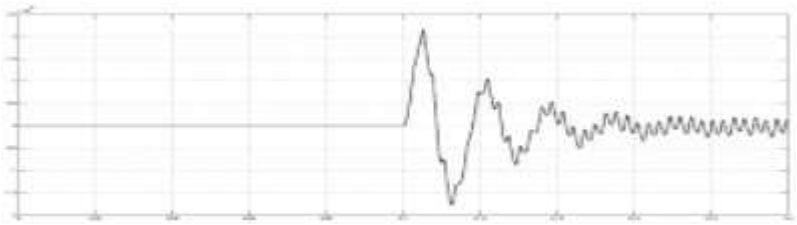

Fig.14 The real power delivered by the storage battery.

During islanded operation, the total generation of the microgrid might not be able to sustain its generation to meet the power demand of the loads. Under such circumstances, consumers participating in DRM will allow the non-critical operation of the microgrid. The second test case demonstrates the islanded operation of the microgrid. In this test case, the microgrid is initially operating in the grid-connected mode for $0 \leq t < 0.1s$. The SB is initially operating in the idle mode till a fault occurs on the upstream network of the distribution grid. The occurrence of fault causes the operation of circuit breaker (CB) at t=0.1s.Fig.15 shows the real and reactive power generated by the distribution grid. At t=0.1s the CB completely isolates the microgrid from the distribution grid so the real and reactive power generated by the grid falls to zero at 0.1s.

When the distribution grid is completely isolated from the micro grid the storage (SB) comes into action as shown in Fig.14. After initiation of the islanding operation at t=0.1s, DG inverter 2 is tasked by the EMS to increase its generation to provide real power about 12.5kW to the loads. With only the main DG and SB supplying the loads, the power imbalance results in a decrease in the system frequency, which is detected by the EMS. To maintain the stability of the microgrid during islanded operation, the shedding of load 3 (P_{L3}=18kW and Q_{L3}=12.3kVAr) is initiated to meet the power demand by the loads.

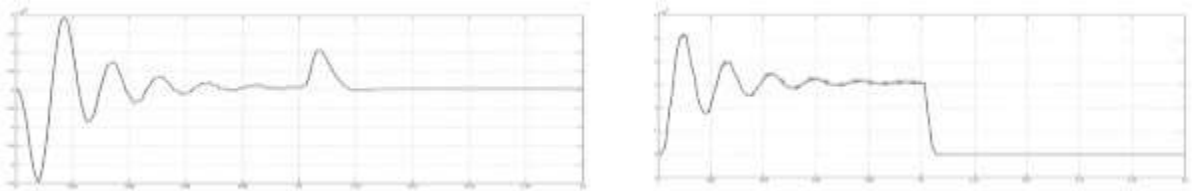

Fig.15 Real (left) and reactive (right) power delivered by the grid.

CONCLUSION

In this paper, a control system that coordinates the operation of multiple DG inverters in a microgrid for grid-connected and islanded operations has been presented. The controller also integrates Kalman filters into the control design to extract the harmonic spectra of the load currents and to generate the necessary references to the controller. By placing an additional DG at the load centre the harmonics in the system reduced and the power quality has improved.

REFERENCES

[1] Aruna Garipelly, "Improvement Of Power Quality Of A Distributed Generation Power System," International Journal of Advances in Engineering & Technology,Vol.5, No.1, pp.276-287, Nov.2012.
[2] I. Kumaraswamy, B. VenkataPrasanth and S.Tarakalyani, "Role of Distributed Generation in Voltage Stability Enhancement," International Journal of Current Engineering and Technology,Vol.4, No.1, pp.60-64,Feb.2014.
[3] M. Coleman, C. K. Lee, C. Zhu and W. G. Hurley, "State -of - charge determination from EMF voltage estimation : Using impedance, terminal voltage, and current for lead-acid and lithium-ion batteries," IEEE Trans.Ind. Electron ., vol. 54, no. 5, pp. 2550–2557, Oct. 2007.
[4] K. T. Tan, P. L. So, Y. C.Chu and M. Z. Q. Chen, "Coordinated Control and Energy Management of Distributed Generation Inverters in a Microgrid," IEEE transactions on power delivery, Vol. 28, No. 2,pp.704-713, April 2013.
[5] Mukhtiar Singh, Vinod Khadkikar, Ambrish Chandra and Rajiv K. Varma, "Grid Interconnection of Renewable Energy Sources at the Distribution Level With Power-Quality Improvement Features," IEEE Transactions On Power Delivery, Vol. 26, No. 1,pp.307-315, Jan 2011.
[6] Toshak Singhal, Akshat Harit, and D N Vishwakarma, "Kalman Filter Implementation on an Accelerometer sensor data for three state estimation of a dynamic system," IJRET, Vol. 1, No. 6,pp.330-334,2012.